

TE-NeXt: A LiDAR-Based 3D Sparse Convolutional Network for Traversability Estimation

Antonio Santo , Juan J. Cabrera , David Valiente , Carlos Viegas , Arturo Gil .

Abstract—Giving an expert system the decision of where to move in a space makes the estimation of traversability a critical task, as there are a multitude of different scenarios. Therefore, it is not a trivial problem to develop models that guarantee an adequate generalisation at the extent of the particular problem to be solved. This paper presents TE-NeXt, a novel and efficient architecture for Traversability Estimation (TE) from sparse LiDAR point clouds based on a residual convolution block. TE-NeXt block fuses notions of current trends such as attention mechanisms and 3D sparse convolutions. TE-NeXt aims to demonstrate high capacity for generalisation in a variety of urban and natural environments, using well-known and accessible datasets such as SemanticKITTI, Rellis-3D and SemanticUSL. Thus, the designed architecture outperforms state-of-the-art methods in the problem of semantic segmentation, demonstrating better results in unstructured environments and maintaining high reliability and robustness in urban environments, which leads to better abstraction. Implementation is available in an open repository to the scientific community with the aim of ensuring the reproducibility of results.

Index Terms—Autonomous mobile robots, LiDAR, Traversability Estimation, 3D Sparse Convolution, Semantic Segmentation.

I. INTRODUCTION

IN a world where autonomous navigation is a reality, the correct estimation of traversability acquires the magnitude of an area of study of its own, as it takes a very important role in the control of the autonomous vehicle in many applications.

The theory of *affordances*, based on animal behavior and their surroundings, as outlined by [1], suggests that the environment provides perceptible cues or *affordances* that guide an observer's actions. Similarly, extending this concept to robotics [2], the robot perceives the environment's capability to be safely traversed, independently of the entity moving through it. These *affordances* might include features such as flat surfaces, clear paths, absence of obstacles, and stable ground.

While traversability estimation has now been widely recognised as a critical capability for mobile robots, it has historically focused on obstacle avoidance. In this traditional context, the primary goal of the robot is to avoid any physical contact with its surroundings and navigate only through open

Antonio Santo, Juan J. Cabrera, David Valiente and Arturo Gil are with the University Institute for Engineering Research, Miguel Hernández University, Avda. de la Universidad s/n, 03202 Elche (Alicante), España (email: {a.santo, juan.cabrera, dvaliente, arturo.gil}@umh.es).

Antonio Santo is with Valencian Graduate School and Research Network of Artificial Intelligence (valGrAI) Camí de Vera S/N, Edificio 3Q, 46022 Valencia, España (email: a.santo@umh.es).

Carlos Viegas is with Univ. of Coimbra, ADAI, Department of Mechanical Engineering, Rua Luís Reis Santos, Pólo II, 3030.788 Coimbra, Portugal (email: carlos.viegas@uc.pt).

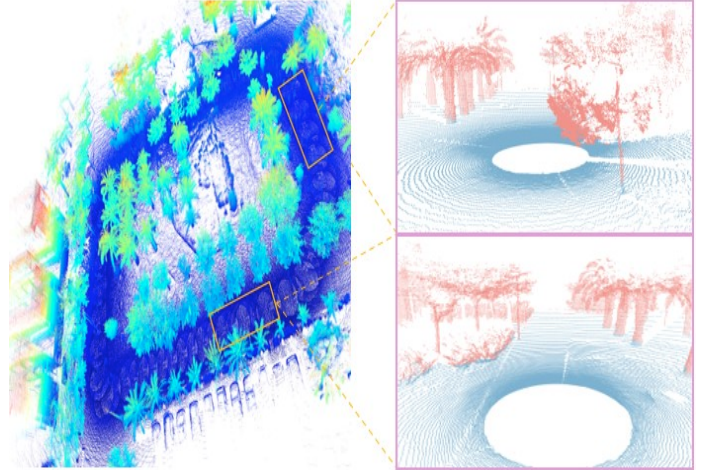


Fig. 1. Point cloud-based traversability estimation. TeNeXt performs inferences about the different instances that conform the map. Each point cloud represents a pose within the 3D map of the environment. Areas identified as potentially traversable are shown in blue and non-traversable areas are shown in red.

spaces, relying on measurements from proximity sensors to detect nearby objects [3]. Afterwards, numerous strategies were developed to ensure safe navigation by means of exteroceptive data; from the creation of alternative representations of space such as 2D [4], [5], 2.5D [6], [7] or occupancy grid maps that enable robot localisation, to the use of supervised learning algorithms, specifically, semantic segmentation on data extracted from RGB, RGB-D cameras [8]–[11], as the traversability analysis problem can also be interpreted as a subclass of the generic multiclass semantic segmentation problem. Despite the limited robustness that these methods exhibit in various outdoor environmental contexts [12], [13], the former approach (extrapolated to a 3D domain) seems to be more suitable for traversability estimation. The evolution of sensor technologies in terms of affordability, accuracy and portability, is leading to a re-evaluation of the methodologies to assess traversability. Specifically, the combination of neural networks with LiDAR sensors has gained popularity. LiDAR's immunity to changes in lighting conditions, unlike optical sensors as cameras, makes it particularly attractive for this purpose.

Thus, in recent years on-road driving has received significant attention in the domain of semantic segmentation, providing databases that, although their primary purpose is not traversability estimation, can be easily adapted to the problem. Nevertheless, on-road driving does not reflect the full extent of

the problem. Off-road environments pose distinct challenges due to their uneven terrain, pronounced textures, and irregular features. The presence of these unique hazards increases the need for the autonomous vehicle to understand its environment at a higher level. Thus, it raises the need to provide a method for several different environments.

This paper presents an environment-independent traversability estimation technique, specifically the design of a deep neural network based on the description of traversable and non-traversable areas regardless of the environment captured by a LiDAR sensor (Figure 1). Several improvements and modifications are proposed based on concepts stated from different aspects of deep learning, in particular convolutional networks and vision transformers (ViT). In addition, significant improvements in both macro and micro design have been carried out. In summary, the main contributions of this paper are:

- TE-NeXt: A novel 3D sparse convolutional neural network architecture for Traversability Estimation. The architecture has been specifically designed and optimised for this problem.
- The design of a new convolutional block: A residual block entirely composed of 3D sparse convolutions that follows the philosophy proposed by ConvNeXt [14] and surpasses the performance of ResNet Blocks [15].

As a result, the proposed network is able to outperform other existing methods in unstructured environments, while maintaining robustness, high precision ratios.

The rest of the paper is organized as follows: Section II describes the current methodologies under which the problem of traversability estimation is addressed. Section III then details the proposed architecture for that purpose. Section IV focuses on the procedure performed in the different experiments and the results obtained. Finally, Section V draws the main conclusions.

II. RELATED WORK

This section provides an overview of the methods that constitute the literature on traversability estimation. It will mention the most relevant deep learning works under which the problem was originally addressed to the current methodologies employed.

The strong emergence of deep learning methods, particularly in the area of computer vision, brought about a paradigm shift, as contrary to traditional traversability estimation methods that based on hand-crafted features and heuristics, these new methods rely on raw sensor data, such as images or point clouds, to learn feature representations. In addition, they attracted a great deal of interest from the research community because of the more visual nature of the information obtained from the environment [16]. Therefore, appearance-based methods became one of the most widely used approaches to this task.

One of the first supervised methods was proposed in [17], where a Multi-Layer Perceptron (MLP) classifier combined with colour and texture features (extracted from RGB images)

was used as a method for automatic classification of road and off-road terrain. However, the methods quickly shifted towards using visual information as input due to the results shown by convolutional networks in image classification tasks. In this context, network architectures such as GA-Nav [8] and DeconvNet [18] emerged. Both only use visual information as input for terrain classification to determine safe areas to traverse and both grouped the semantic segmentation into 6 and 5 classes respectively.

In addition to methods that use visible spectrum images, methods have also been developed that rely on the infrared spectrum to estimate the traversability of the environment in order to avoid low-light situations such as night, backlight, haze, etc... Pioneering works such as [19] present a convolutional neural network (CNN) for traversability estimation, and compare the optimal way to implement multi-model data fusion, now known as early or late fusion. URTSegNet [20], inspired by methods that perform segmentation in infrared images [21], proposes a real-time neural network including two different branches to extract spatial detail and contextual features.

Progress in high-resolution data processing [22] made it possible to extrapolate the concept of traversability, previously approached from a two-dimensional point of view, to a three-dimensional domain. Point clouds produced by LiDAR sensors have served as the basis for traversability estimation methods in a 3D environment [23]–[25], although pre-processing is required.

A common practice in a three dimensional context is 3D voxel partition, in works such as [26], [27] the authors represent the point cloud as a 3D voxel occupancy map. This voxel representation avoids the need for commonly used elevation maps, which are prone to error in the presence of overhanging obstacles and in multi-storey or low ceiling scenarios. Apart from the internal representation of the environment, they proposed a 3D sparse encoder-decoder that exploits the sparsity of the voxel representation for efficient computation. However, there are different ways of representing point clouds, from [28] where they are arranged in a multilevel polar grid, which naturally takes into account the non-uniform density of point clouds, to cylindrical voxelisation [29] based on the cylindrical coordinate system, which adjusts to the variable dispersion of the LiDAR point cloud.

As with 2D vision, methods that fused input information of different nature were developed in the 3D context. One of the most common proposals is the merging of surface normals extracted from LiDAR data with RGB images [30]–[32]. All of them utilize multi-modal fusion of RGB images and geometric information derived from LiDAR point clouds. The architectures proposed employ transformer-based encoder blocks to extract features from the input modalities. This allows them to leverage the advantages of transformers in modeling long-range dependencies and global context.

Similarly, other approaches have combined the point clouds with data collected from the interaction of the vehicle with the environment, not as a fusion of input data but to establish training labels. Works such as [33]–[35], automatically generate

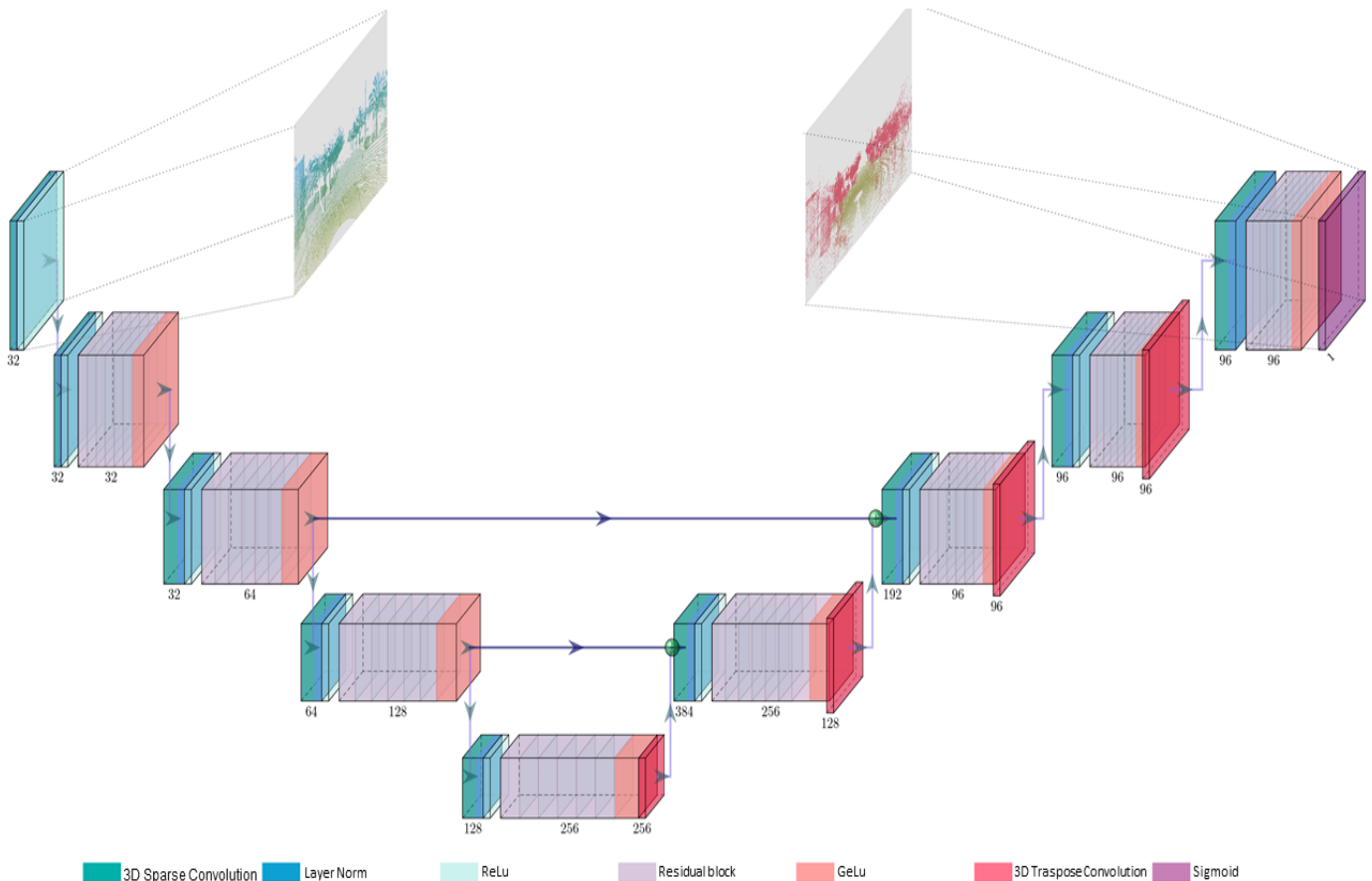


Fig. 2. Traversability Estimation framework overview. A detailed illustration of the proposed TE-NeXt architecture, following the original scheme of the U-Net network [36]. A LiDAR point cloud is subjected to the extraction of descriptors at varying resolutions on the left-hand side of the image. Once the information has been encoded, the initial dimensions are recovered in order to obtain a label for each point.

training labels from proprioceptive data. This kind of approach is known as self-supervised traversability, where labels are generated from past driving trajectories by labeling regions traversed by the vehicle as highly traversable. The wheel-contact points are projected into image coordinates and filtered for occlusions using LiDAR points. Unsupervised LiDAR denoising is performed for robust labeling in unstructured environments.

Finally, this paper presents TE-NeXt, an architecture based on a sparse variant of the U-Net neural network [36], modified and improved for its application to traversability and non-traversability verification by approaching it as a pointwise point cloud semantic segmentation problem. The proposed architecture requires a point cloud as input, as some of the methods mentioned in this section, and the feature extraction at different scales is given in the residual block designed taking notions from the two current trends such as vision Transformers and ConvNext [14] philosophy. TE-NeXt demonstrates robustness in structured environments, with performance in natural outdoor environments at the core of the network design, outperforming state-of-the-art methods in these environments.

III. TE-NeXt: AN ARCHITECTURE FOR TRAVERSABILITY ESTIMATION

TE-NeXt is a novel sparse convolutional network designed for 3D semantic segmentation of point clouds, with a specific focus on traversability estimation. TE-NeXt builds upon the U-Net style architecture [36], replacing the standard residual blocks, introduced by classical ResNet networks [37], with a customised block inspired by the ConvNeXt [14] design principles. What sets TE-NeXt apart from recent work in this domain is its aim to learn a more general, high-level understanding of the environment that is not tied to specific settings or robotic platforms.

A. Network Architecture Overview

Traversability estimation can be considered a semantic segmentation problem. Considering a simple point cloud as input, discriminant features could be extracted by preprocessing the data. The income's internal representation follows the methodology used by 3D sparse convolutional library, Minkowski Engine [38]. It is defined by $I = \{(\vec{T}_c, \vec{T}_f), l_i\}$, where $\vec{T}_c = (x_i, y_i, z_i)$ comprises those coordinates provided by the collimated beams of the LiDAR sensor, ignoring the

spaces where there is no information based on sparse matrix principles, whereas \vec{T}_f describes point-wise features and l_i indicates the traversability condition.

As previously stated, the focus of recent works is on the identification of environmental attributes that facilitate the discernment of traversable from non-traversable areas. However, in other domains such as large-scale place recognition, which a priori generalisation is a fundamental requirement, the features are initiated as a vector of 1's for those non-empty voxels [39], [40]. According to this view, the method presented in this paper continues such approach as it aims to optimise the abstraction process in every possible environment without favouring it in any of them.

Next, we provide a description of the TE-NeXt architecture, depicted in Figure 2. The proposed network adopts a hierarchical structure analogous to the U-Net [36], which is an encoder-decoder configuration, with the spatial dimensions initially reduced through strided convolution operations. This enlarges the receptive field size of the neurons at deeper layers, enabling them to capture a more extensive contextual information from the input. Following each of these operations, a normalisation layer, LayerNorm, and an activation function, ReLU, are employed for each level of network resolution. The latter is a common technique in convolutional networks to learn complex, non-linear mappings between inputs and outputs. Conversely, the utilisation of a normalisation technique that is not commonly employed in classical convolutional networks is justified by the promising outcomes observed in vision Transformers. The main reason why it has proved so effective is its invariance with respect to the batch size, since it is not usually possible to process large amounts of data simultaneously in a three-dimensional domain.

Subsequently, the spatial dimensions are incrementally augmented through upsampling operations, such as transposed convolutions. To compensate for the loss of spatial details during encoding, skip connections are employed to concatenate feature maps from the encoder path with those in the decoder path at the same resolution level. Unlike U-Net and applying the same policy of [26] reducing the number of skip connections to only the lower layers, it helps reduce false positive predictions, likely because the decoder does not have to predict many forwarded features from the encoder. Using fewer skip connections seems to act as a form of regularization and improves overall traversability prediction performance on its task. As a result, the neurons in the final layers of the decoder have a large effective receptive field, capturing both global context and local details. Finally, as a decoder, the network output holds the same dimensions as the input data, providing a probability value obtained via a Sigmoid function as the final layer.

B. TE-NeXt residual block

The core innovation in TE-NeXt lies in its custom residual block. This block draws inspiration from the design principles of ConvNeXt [14], a Convolutional Network architecture which has inspired numerous works that constitute the current state-of-the-art on free space detection in images [32].

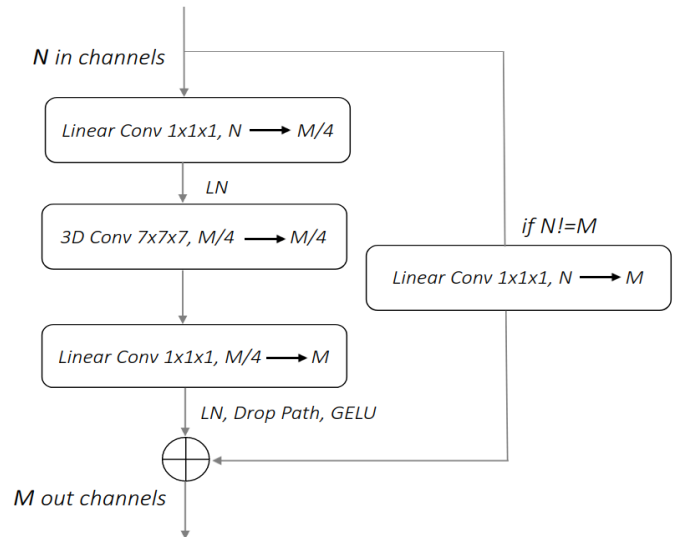


Fig. 3. The structure of the proposed residual block TE-NeXt.

It incorporates several key ideas from vision Transformers while maintaining the simplicity and efficiency of standard ConvNets. TE-NeXt aspires to learn rich, generalizable feature representations from large-scale 3D point cloud data. The residual block is depicted in Figure 3.

The N -channel input first passes through a $1 \times 1 \times 1$ convolutional layer that reduces the channels by a factor of 4, alleviating the computational complexity and memory requirements of subsequent layers. It operates on each channel independently, permitting learning channel-specific filters and weights. This allows the network to selectively suppress redundant information across channels. It then passes through a 3D convolutional layer with a $7 \times 7 \times 7$ kernel, maintaining the input dimensions of the layer.

Next, another linear convolution layer increases the channels back to the desired output. In essence, the final $1 \times 1 \times 1$ convolution allows the residual block to: i) restore the original channel dimensionality after the bottleneck layers, ii) increase representational power, iii) perform projection mapping. Finally, if the input and output dimensions are equal ($N=M$), the input is added to the output via a skip connection before the normalization layer, the regularization technique applied (drop Path [41]) and a Gaussian Error Linear Unit (GeLU) [42]. Regarding the activation function employed, GeLU is smoother than Rectified Linear Unit activation (ReLU) and is utilized in the most advanced Transformers. This skip connection allows gradients to flow more easily during back-propagation, mitigating the vanishing gradient problem in very deep networks. Furthermore, the residual block can learn an identity mapping when needed, making it easier to optimize.

IV. EXPERIMENTS

A. Datasets

A set of publicly available databases has been used for training, validation and testing of the neural network design, in particular:

- SemanticKITTI [43]: A large-scale dataset for semantic scene understanding of LiDAR sequences. It is based on the KITTI Vision Odometry Benchmark [44] and provides dense point-wise annotations for the complete 360° field-of-view of the Velodyne HDL-64E LiDAR sensor used in the KITTI dataset. It consists of over 43,000 LiDAR scans from 22 sequences of the KITTI Odometry Benchmark, with over 4 billion points in total. The sequences cover a variety of highly structured environments including city streets, residential areas, highways, and countryside roads.
- Rellis-3D [45]: Multimodal dataset designed for off-road robotics and autonomous navigation research, serving as an extraordinary complement to other existing autonomous driving datasets that focus on urban scenes. It consists of 13,556 point clouds divided into 4 distinct sequences captured by means of an OS1-64 LiDAR.
- SemanticUSL [46]: Comprises 16,578 unlabeled LiDAR scans, which are intended for unsupervised domain adaptation training, and an additional 1,200 labeled scans for evaluation purposes. SemanticUSL adopts the same data format and ontology as the well-established SemanticKITTI dataset, making it convenient for researchers to utilize in their domain adaptation studies. The data collection process for SemanticUSL involved the use of a Clearpath Warthog robotics platform equipped with an Ouster OS1-64 LiDAR sensor.

The datasets contain around 25 to different semantic labels that a point can be assigned, such as bush, mud, asphalt, sidewalk, etc. The condition labels were reclassified based on its traversability, resulting in only two classes: "traversable" and "non-traversable". The classes converted to "traversable" include sidewalk, asphalt, low vegetation or grass, dirt, cement, and mud. The "non-traversable" class comprises tree, person, car, truck, building, and others. This binary categorization was done by considering the ability of a robot to safely navigate across the different surface types.

B. Training and evaluation process

Since the intention is to develop a multimodal model without giving preference to any of the environments described above, a prior selection has been carried out on the training to ensure equivalence. As Rellis-3D is not as extensive as SemanticKITTI, it was not used in its entirety. Specifically, 10,700 clouds of unstructured environments have been selected, belonging to 3 of the 4 sequences in Rellis-3D. The first 4 SemanticKITTI sequences have been selected, thus ensuring 11,100 clouds of structured environments. In addition, the validation and testing process have been carried out with sequences from both datasets, adding all the SemanticUSL data in order to assess the degree of generalisation of the neural network in a never-before-seen environment.

Table I specifies the hyperparameters and settings used to train the model from randomly initialized weights. The optimizer used AdamW with an initial Learning Rate (LR) of 5e-3 along to Cosine Annealing scheduler causes the LR

TABLE I
ENVIRONMENTAL-INDEPENDENT TRAINING SETTING

Scratch	
Config	Value
Optimizer	AdamW
Scheduler	Cosine
Criteria	Binary Cross Entropy
Learning Rate	5e-3
Weight decay	0.05
Batch size	5
Datasets	Sem.KITTI, RELLIS-3D
Quantization scale	0.2
Warmup epochs	80
Termination criteria	F1 score

to follow a cosine function over the same training epoch. It performs periodic "warm restarts" where the learning rate is reset back to the initial value after a certain number of batches. This simulates the restarting of the learning process using the weights from the previous run as a good starting point. The periodic restarts help the model escape from local minima and saddle points. Since the model has been trained for a binary segmentation task, the F1 score is a suitable metric for imbalanced datasets and considers both: precision (the proportion of true positive predictions among all positive predictions) and recall (the proportion of true positive predictions among all actual positive instances). This ensures that the model is not optimizing for one metric at the expense of the other. Furthermore, if the F1 score on the validation set stops improving or starts to decrease, training can be stopped early to prevent overfitting and obtain a model with good generalization.

C. Ablation study

This section presents the roadmap followed during the development of the architecture proposed in this paper, being the starting point the MinkU-Net34C architecture. For this purpose, a first distinction will be made in three blocks. The first will provide a study of the effect of input features on network performance. The second one will present the design steps that affect the structure of the neural network. Subsequently, the methodology employed in the design of the residual block, which represents the primary innovation of this work, will be explained.

Out of many experiments, those successful were classified according to different design principle, as shown in Figure 4. Each bar represents the performance of the different models on the Rellis-3D dataset, in terms of two metrics considered relevant to the task of traversability estimation: F1 score and precision. They are considered relevant mainly because of the class imbalance and the importance of false negatives/positives. Precision measures the model's ability to avoid matching non-traversable areas as traversable (avoid false positives), which is crucial for safety. Recall measures the ability of the model to detect all traversability areas (avoidance of false negatives), which is important for efficient navigation. The F1 metric combines precision and recall into a single score, allowing assessing the balance between the two of them.

1) Input data:

Features: In contrast to 2D convolutions, where the input and output tensors have a fixed number of feature dimensions, typically called channels (e.g. RGB channels for images), 3D sparse convolutions allow sparse tensors to have an arbitrary number of feature dimensions. Each non-zero element in the sparse tensor can have a feature vector of arbitrary length. Therefore, as a first step, a study of the possible most discriminating features for estimating traversability was carried out. Among the most representative are those shown in Figure 4 (experiments A, B, C, referred to in Table II). However, the vector of 1's was chosen as the main one for future modifications because it is equally discriminant and at the time of inference it represents an improvement in efficiency.

2) Global Design:

Cardinality: This term was introduced by ResNext [47], and refers to the number of parallel branches within each block. In relation to this, numerous configurations have been evaluated. Firstly, the MinkU-Net34 network with (2,3,4,6,2,2,2,2,2) branches per block. In order to reduce the number of model parameters it was decided to test the MinkU-Net18 and MinkU-Net14. These smaller versions, especially MinkU-Net14, have significantly fewer branches in each convolutional block compared to MinkU-Net34. Fewer branches means fewer filters and therefore fewer trainable parameters in the model. In summary, by carefully exploring smaller architectures, it was possible to find very efficient MinkU-Net configurations that achieve a good compromise between model size and performance. It shows that it is often possible to substantially compress neural networks without sacrificing their ability to learn and generalise. This change does not represent an improvement in terms of performance but does represent an improvement in efficiency as it will be shown in Table VI.

Skip connections: Unlike the U-Net architecture [36], TeNext presents a variation in the connections that are made between the respective parts of the encoder and decoder. As it has already been seen in works such as [26], [27], it does not seem appropriate for the traversability estimation task to maintain the original connections proposed by U-Net. Thus, this change in the global design of the network allows to obtain a 5% improvement with respect to its predecessor, experiment E, and a 3% improvement with respect to the initial neural network F1 metric, MinkU-Net, experiment D and C.

Modifications in the residual block: Previously, the residual block was the original residual block of ResNetv1 [48], so the necessary modifications were made to update it to its second version, replacing the 2D convolution operations with linear convolutions. This modification is represented in the Figure 4 by the experiment G mentioned in the Table II and implies an increase of 2% in terms of F1.

3) Micro Design:

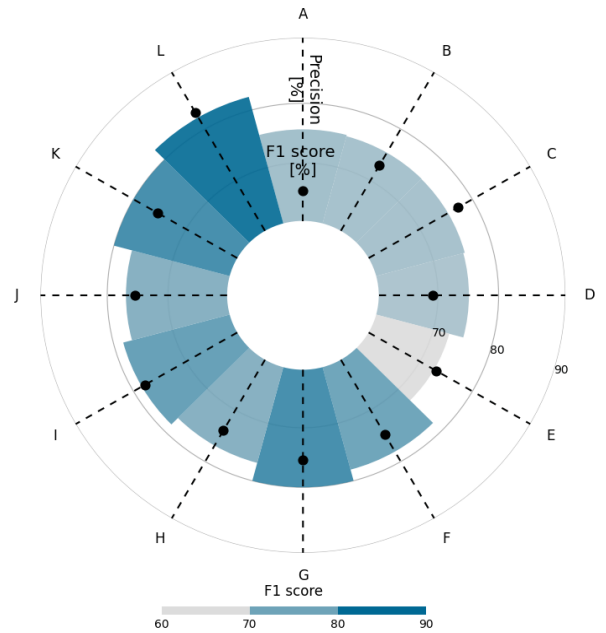


Fig. 4. Design process of the proposed architecture, TE-NeXt, starting from a base MinkU-Net34C. All experiments are detailed in Table II.

TABLE II
EXPERIMENTAL MODIFICATIONS CARRIED OUT DURING THE DESIGN OF THE PROPOSED ARCHITECTURE, FOR WHICH PERFORMANCE IS PRESENTED IN FIGURE 4

Steps	Experimental Modifications
A	Features: $\vec{T}_c = (x_i, y_i, z_i)$
B	Features: $\vec{T}_c = (x_i, y_i, z_i) + \vec{T}_n = (n_x, n_y, n_z)$
C	Features: One's Vector
D	Cardinality: (2,3,4,6,2,2,2,2) \rightarrow (1,1,1,1,1,1,1,1)
E	4 skip connections \rightarrow 3 skip connections
F	3 skip connections \rightarrow 2 skip connections
G	Resnet Residual Block \rightarrow Inception-ResNetv2 Residual Block
H	Fewer Activations
I	Kernel Size: 5 \rightarrow 7
J	ReLU \rightarrow GeLU
K	Batch Norm \rightarrow LayerNorm
L	Drop Path

Fewer activations: While activation functions after each convolutional layer is the most common approach, there are specific architectures and scenarios where selectively removing or moving them could make sense, like for computational efficiency or parameter reduction in mobile networks. However, this requires careful experimentation as haphazardly removing activations especially in deeper layers could hurt performance by limiting the non-linearity and representational power of the network.

Kernel size: Traditional CNNs typically use small kernels, Transformer-based architectures and Transformer-

inspired CNN designs often employ much larger kernels, from 7×7 and beyond. This allows them to capture longer-range dependencies and broader context, contributing to their strong performance on various vision tasks. Hence, as the Figure 4 shows, the experiment *I* referenced in the Table II leads to a 1% improvement with respect to F1 metric.

Normalization: Likewise to activation functions, it has become common practice to place operations that normalise the activations of each layer because of their multiple benefits in the learning process. However, Batch-Norm [49] computes statistics (mean and variance) over the whole batch, so its effectiveness may decrease with small batch sizes. LayerNorm [50] avoids this problem by normalising the statistics per instance. This means it is not affected by batch size. In summary, LayerNorm’s robustness to small batch sizes, its applicability to recurrent and sequential models, and its consistency between training and inference, explain its superior performance as shown in experiment *K* in Figure 4.

GeLu activation function. The ReLU has been the most popular activation function in deep learning due to its simplicity and efficiency. However, recent advanced Transformer models have started using the GELU instead. GELU is a smoother variant of ReLU that can enable better training of deep networks by reducing issues like vanishing gradients and allowing useful gradients for negative input values. The incorporation of this technique in the block resulted in a 2% increase in yield, which is reflected in experiment L.

Regularization technique. Dropout and drop-path are regularization techniques used in training deep neural networks to prevent overfitting and to improve generalization performance. Dropout randomly drops out (sets to zero) units in a layer during training, while drop-path randomly drops out entire paths or connections between layers. This prevents units or paths from relying too much on each other, forcing them to individually be more robust.

D. Results

In this section a performance comparison of the proposed method and models from the literature of the semantic segmentation problem will be presented. Aiming at providing a fair comparison, all models have been adapted to the traversability estimation problem, trained from scratch and validated under the same conditions and data. The original codes of the compared methods have been adapted for the study and had to be modified in order to establish the comparison.

The following comparison has been made with methods covering the same problem from different approaches: from a multi-layer perceptron approach, through the well-known 2D convolutional networks to the novel sparse convolutions that allow efficient handling of three-dimensional data. Since TE-NeXt has been developed based on the performance of modifications from the base architecture design, in unstructured environments, as discussed IV-C Section, the comparison has been divided into 3 different categories:

1) *Performance in structured environments:* Table III presents the results of several semantic segmentation methods for the estimation of traversability in urban environments, using the validation sequence of the SemanticKITTI dataset. The proposed method TE-NeXt, achieves the best overall performance with a F1 score of 96.0%. This is supported by the nature of the metric itself as it combines precision and recall, taking into account both false positives and false negatives.

False positives in autonomous driving imply an inherent risk, not only to the vehicle itself but also to its environment and occupants. This critical aspect is reflected in metrics such as mIoU (mean Intersection over Union for traversable and non-traversable areas) and TNR (True Negative Rate), which assess the model’s ability to correctly identify non-traversable areas. The proposed TE-NeXt method achieves the same TNR as state-of-the-art techniques such as Cyl3D, PVKD and SalsaNeXt. These advances, although they may seem modest, have significant implications for safety by reducing the false positive rate in the segmentation of obstacles and inaccessible areas.

2) *Performance in natural environments:* Table IV presents the results of various semantic segmentation methods for traversability estimation in natural environments using the Rellis-3D dataset. Unlike in urban environments, it is remarkable the good performance of the most classic method, PointNet, outperforming more modern methods in most of the metrics extracted.

The proposed architecture, TE-NeXt, exhibits the best overall performance, with an F1 score of 82.0%, an accuracy of 88.3% and an mIoU of 77.0% for the non-risk and potentially dangerous areas for the robot’s integrity. This outperforms other MinkU-Net-based approaches such as MinkU-Net+ConvNeXt, as well as methods that transform the input cloud given by a LiDAR to an image using projective geometry such as SqueezeSegV3 and SalsaNeXt. In addition to a high mIoU for traversable and non-traversable areas, it achieves a significant true positive rate (TPR) of 81.3%, indicating a good ability to correctly identify traversable areas. At the same time, it has a high true negative rate (TNR) of 91.8%, demonstrating its effectiveness in discarding non-traversable areas.

By contrast, compared to results in urban environments (Table III), the overall performance is lower for all methods in the Rellis-3D dataset. This poses that semantic segmentation for traversability estimation in natural environments is a more challenging task due to the higher variability and complexity of scenes. Since there are no references to the evaluation of some of the mentioned methods in unstructured environments, it has been decided not to include them in the following Tables.

3) *Performance in mixed environments:* Table V presents the results of various semantic segmentation methods for the estimation of traversability in outdoor environments. Contrarily to previous tests, this is a fully employed dataset for testing purposes, considering semi-structured environments.

Regarding the performance of the proposed model, it is shown that it is comparable with the best methods in terms

TABLE III
TRAVERSABILITY ESTIMATION PERFORMANCE OF SEMANTIC SEGMENTATION METHODS
IN URBAN ENVIRONMENTS.

Urban envs. Sem. seg Methods	SemanticKITTI					
	Voxel	F1 score	Accuracy	mIOU	TPR	TNR
PointNet [51]	-	93.50	93.70	88.1	96.50	91.10
PointNet++ [52]	-	83.36	84.28	72.45	81.15	87.52
SqueezeSegv3 [53]	-	96.5	97.6	94.9	96.6	98.1
SalsaNeXt [54]	-	95.9	97.30	94.25	95.0	98.5
P-SVM [28]	-	89.2	91.7	83.9	89.0	93.4
RN++ [55]	-	94.0	95.4	90.7	93.2	96.8
Cyl3D [29]	-	95.8	96.8	93.45	95.3	97.7
PVKD [56]	-	95.9	96.9	93.65	95.6	97.7
MinkU-Net [38]	0.2	93.7	95.20	90.05	94.0	93.8
MinkU-Net [38]+ ConvNeXt [14]	0.2	94.6	95.2	90.85	97.6	94.4
TE-NeXt (ours)	0.2	96.0	96.3	92.90	94.7	97.7

TABLE IV
TRAVERSABILITY ESTIMATION PERFORMANCE OF SEMANTIC SEGMENTATION METHODS IN NATURAL ENVIRONMENTS.

Natural envs. Sem. seg Methods	Rellis-3D					
	Voxel	F1 score	Accuracy	mIOU	TPR	TNR
PointNet [51]	-	80.3	87.2	74.90	76.43	92.8
PointNet++ [52]	-	58.9	50.2	32.1	45.6	67.0
SqueezeSegv3 [53]	-	70.8	89.1	71.15	65.3	95.1
SalsaNeXt [54]	-	73.5	90.0	73.30	68.9	95.5
MinkU-Net [38]	0.2	75.8	83.3	69.15	80.0	84.9
MinkU-Net [38] + ConvNeXt [14]	0.2	78.3	85.9	72.75	77.8	89.8
TE-NeXt (ours)	0.2	82.0	88.3	77.00	81.3	91.8

TABLE V
TRAVERSABILITY ESTIMATION PERFORMANCE OF SEMANTIC SEGMENTATION METHODS IN MIXED ENVIRONMENTS.

Mixed envs. Sem seg Methods	SemanticUSL					
	Voxel	F1 score	Accuracy	mIOU	TPR	TNR
PointNet [51]	-	90.2	90.1	82.0	94.9	85.7
PointNet++ [52]	-	87.13	87.0	77.10	91.4	83.1
SqueezeSegv3 [53]	-	91.5	95.6	89.4	97.9	98.25
SalsaNeXt [54]	-	95.0	97.3	93.5	95.9	97.8
MinkU-Net [38]	0.2	94.3	94.4	89.35	98.1	91.0
MinkU-Net [38]+ ConvNeXt [14]	0.2	95.0	95.1	90.6	98.3	92.2
TE-NeXt (ours)	0.2	95.0	95.0	90.6	97.9	92.5

of F1 score, even though all the modifications made with a bias towards performance in natural environments. Methods such as SqueezeSegV3 and SalsaNext show very competitive performance, especially in terms of accuracy and TNR. They significantly outperform PointNet and PointNet++.

The proposed TE-NeXt model demonstrates impressive performance, achieving an F1 score and accuracy of 95.0%, along with a high mIoU of 90.6%. Moreover, TE-NeXt exhibits a remarkable ability to accurately identify traversable regions, as evidenced by its high true positive rate of 97.9%. Simultaneously, it proves high effectivity in excluding non-traversable areas, boasting a true negative rate of 92.5%. These results showcase the model's robustness and reliability in distinguishing between traversable and non-traversable terrain.

E. Qualitative Evaluation

Figure 5 presents the results in a visual form, where the different colours refer to the success or failure cases for each class considered: true positives (blue), true negatives (red), false positives (purple), false negatives (yellow). The complete inference of the test sequences belonging to the aforementioned datasets is publicly available on YouTube¹.

Figure 5a shows the predictions of the proposed architecture on a cloud in an unstructured environment. On the one hand, it can be seen that the points classified as traversable (false positives) are located in the boundaries of the different geometries detected by the LiDAR, the source of this error being the naturalisation of the algorithm itself, which discretises the environment into voxels. As for the false negatives, two situations are evident: i) those that appear in the right part

¹<https://www.youtube.com/watch?v=mn6NKInxjOs&t=122s>

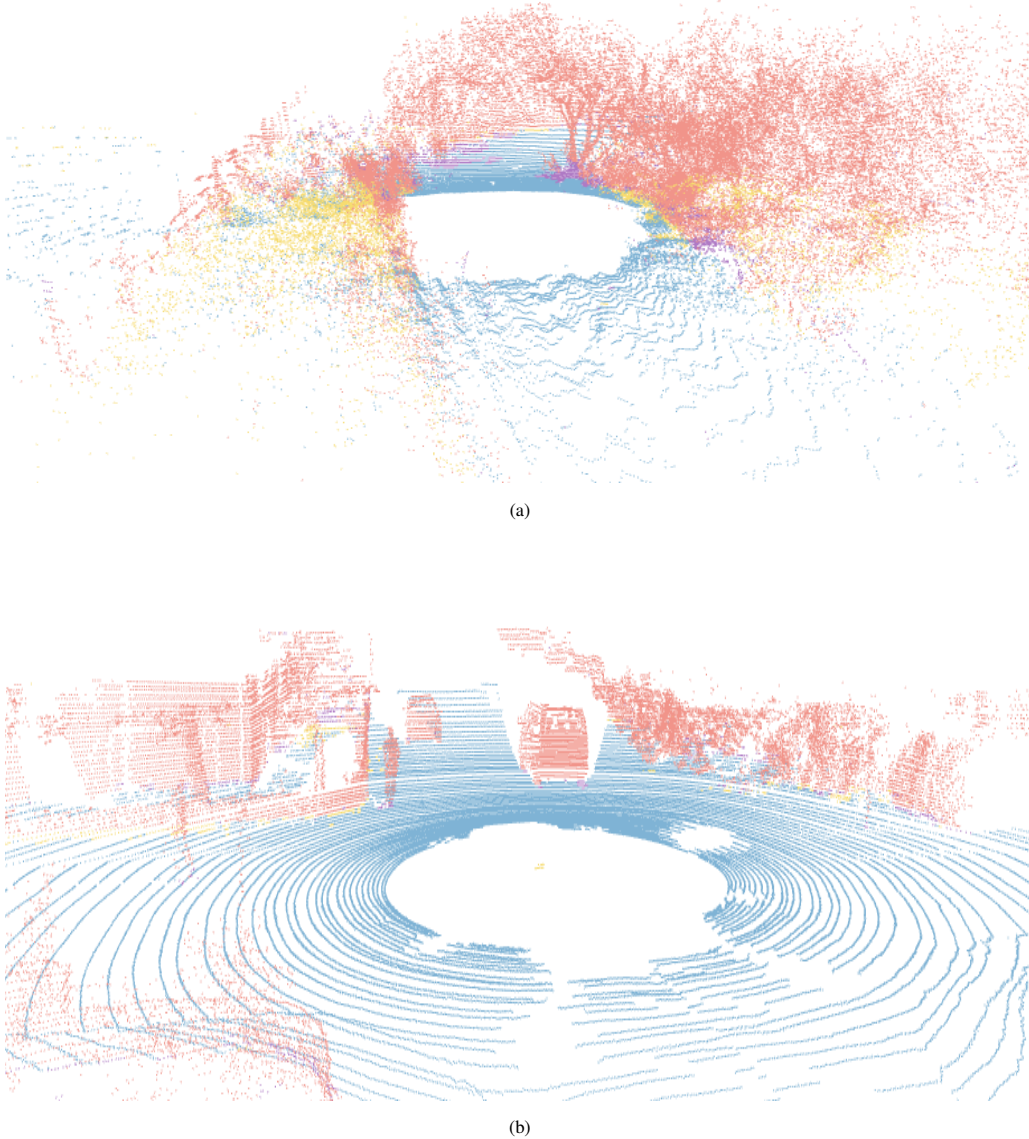


Fig. 5. Te-NeXt architecture inference visual representation. ■: true positives (TP). ■: true negatives (TN). ■: false positives (FP). ■: false negatives (FN). (a) Inference on a point cloud from the Rellis-3D dataset. (b) Inference on a point cloud from the SemanticKITTI dataset.

of the image are errors due to the diffuse geometry of the environment, ii) the points that appear to be classified as false negatives are actually due to an error in the labelling of the data, since this part of the environment cannot really be traversed.

Figure 5b shows the predictions of the proposed architecture on a cloud in an urban environment. In this type of environment, as can be seen in the interpretation of results, the inference of the network is much more accurate, there are hardly any errors, and sources of error such as false positives occur for the same reasons mentioned above.

F. Implementation details

All the experiments have been tested on an Intel Core™ i9-10900X, $20 \times 3.70\text{GHz}$, 128GB RAM platform with a NVIDIA RTX 3090 with 24GB VRAM graphic card. The

neural network model is implemented using the Minkowski Engine [38], Pytorch and it can be easily integrated into ROS NOETIC. Reproducibility is ensured by a standardized report altogether with the dataset, which are publicly available at Github².

Table VI provides an informative comparison of key efficiency metrics for the methods compared above. The results highlight the substantial differences in model size, memory needs and latency that can arise from architecture choices. Concerning the size of the model, it can be seen how Te-NeXt achieves one of the objectives that was important in its design, the simplification of the model without having an effect on its performance, since many models make an efficiency-for-performance trade-off.

²<https://github.com/ARVCUMH/te-next>

Methods using 3D convolutions (MinkU-Net34C, MinkU-Net+ConvNeXt, TE-NeXt) tend to have lower training memory requirements compared to those using MLP or 2D convolutions, despite having more parameters in some cases. This suggests 3D convolutions may be more memory efficient during training.

V. CONCLUSION

This paper presented TE-NeXt, a point cloud traversability estimation method based on a novel 3D sparse convolutional neural network. It is an architecture inspired by MinkU-Net, whose main contributions lie in the new convolutional residual block. It is proved how an architecture based entirely on convolutions in a three-dimensional domain provides the most robust response regardless of the environment being evaluated, compared to other methods. Emphasising the importance of the proposed residual block, which allows to employ large 2D kernel sizes to model long-range dependencies combined with linear convolutions that reduce computational cost, allow cross-channel mixing, adjust dimensions for skip connections, and provide learnable feature fusion. The proposed architecture exploits an efficient volumetric representation through MinkU-Net [36] and the deep learning capabilities of techniques that have shown robustness in semantic segmentation problems, such as vision Transformers [57] and ConvNeXt [14].

Furthermore, the comparison results presented in this work validate the effectiveness of the proposed approach, TE-NeXt, for traversability estimation in highly natural environments, since the network outperform state-of-the-art methods achieving the best results in terms of model stability (F1 score), mIOU and TPR. Similarly to the behaviour presented by the other state-of-the-art methods with natural environments, the approach shows slightly lower performance in such context. There is therefore a need for further research and improvement of methods to cope with the increasing complexity of natural scenes. Moreover, the network shows similar results to the best semantic segmentation methods in urban environments.

Future work will include the addition of visual information through a LiDAR-camera calibration, which will allow visual features to be introduced into the sparse tensors. Possibly with the aim of mitigating the main problem of supervised learning, the content of the labelled data, we will investigate the exposure of a hybrid method that allows continuous estimation of traversability.

VI. ACKNOWLEDGMENTS

This work has been funded by the ValgrAI Foundation, Valencian Graduate School and Research Network of Artificial Intelligence through a predoctoral grant. In addition, this publication is part of the project TED2021-130901B-I00, funded by MCIN/AEI/10.13039/501100011033 and by the European Union “NextGenerationE”/PRTR” and of the projects PROM-ETEO/2021/075 funded by the Generalitat Valenciana. The authors acknowledge Fundação para a Ciência e a Tecnologia (FCT) for its financial support via the project LAETA Base Funding (DOI:10.54499/UIDB/50022/2020).

TABLE VI
COMPARISON OF SEMANTIC SEGMENTATION METHODS IN TERMS OF EFFICIENCY

Method's Efficiency	Params	Type	Training Memory	Inference Latency
PointNet [51]	3.5M	MLP	13GB	11 ms
PointNet++ [52]	0.9M	MLP	13.6GB	250 ms
SqueezeSegv3 [53]	9.2M	2D	37.8GB	29 ms
SalsaNeXt [54]	6.7M	2D	11.2GB	8 ms
MinkU-Net [38]	37.9M	3D	6.1GB	53ms
MinkU-Net [38]+ConvNeXt [14]	66.4M	3D	8.7GB	78 ms
TE-NeXt (ours)	5.4M	3D	5.4GB	31 ms

REFERENCES

- [1] J. J. Gibson, “The theory of affordances,” *Hilldale, USA*, vol. 1, no. 2, pp. 67–82, 1977.
- [2] E. Şahin, M. Cakmak, M. R. Doğar, E. Uğur, and G. Üçoluk, “To afford or not to afford: A new formalization of affordances toward affordance-based robot control,” *Adaptive Behavior*, vol. 15, no. 4, pp. 447–472, 2007.
- [3] O. Khatib, “Real-time obstacle avoidance for manipulators and mobile robots,” *The international journal of robotics research*, vol. 5, no. 1, pp. 90–98, 1986.
- [4] H. Moravec and A. Elfes, “High resolution maps from wide angle sonar,” in *Proceedings. 1985 IEEE international conference on robotics and automation*, vol. 2. IEEE, 1985, pp. 116–121.
- [5] W. Hess, D. Kohler, H. Rapp, and D. Andor, “Real-time loop closure in 2d lidar slam,” in *2016 IEEE international conference on robotics and automation (ICRA)*. IEEE, 2016, pp. 1271–1278.
- [6] D. Langer, J. Rosenblatt, and M. Hebert, “A behavior-based system for off-road navigation,” *IEEE Transactions on Robotics and Automation*, vol. 10, no. 6, pp. 776–783, 1994.
- [7] C. Ye and J. Borenstein, “A method for mobile robot navigation on rough terrain,” in *IEEE International Conference on Robotics and Automation, 2004. Proceedings. ICRA '04. 2004*, vol. 4. IEEE, 2004, pp. 3863–3869.
- [8] T. Guan, D. Kothandaraman, R. Chandra, A. J. Sathymoorthy, K. Weerakoon, and D. Manocha, “Ga-nav: Efficient terrain segmentation for robot navigation in unstructured outdoor environments,” *IEEE Robotics and Automation Letters*, vol. 7, no. 3, pp. 8138–8145, 2022.
- [9] S. Matsuzaki, K. Yamazaki, Y. Hara, and T. Tsubouchi, “Traversable region estimation for mobile robots in an outdoor image,” *Journal of Intelligent & Robotic Systems*, vol. 92, pp. 453–463, 2018.
- [10] S. Palazzo, D. C. Guastella, L. Cantelli, P. Spadaro, F. Rundo, G. Muscato, D. Giordano, and C. Spampinato, “Domain adaptation for outdoor robot traversability estimation from rgb data with safety-preserving loss,” in *2020 IEEE/RSJ International Conference on Intelligent Robots and Systems (IROS)*. IEEE, 2020, pp. 10 014–10 021.
- [11] B. Gao, S. Hu, X. Zhao, and H. Zhao, “Fine-grained off-road semantic segmentation and mapping via contrastive learning,” in *2021 IEEE/RSJ International Conference on Intelligent Robots and Systems (IROS)*. IEEE, 2021, pp. 5950–5957.
- [12] X. Xiao, B. Liu, G. Warnell, and P. Stone, “Motion planning and control for mobile robot navigation using machine learning: a survey,” *Autonomous Robots*, vol. 46, no. 5, pp. 569–597, 2022.
- [13] J. Frey, M. Mattamala, N. Chebrolu, C. Cadena, M. Fallon, and M. Hutter, “Fast traversability estimation for wild visual navigation,” *arXiv preprint arXiv:2305.08510*, 2023.
- [14] Z. Liu, H. Mao, C.-Y. Wu, C. Feichtenhofer, T. Darrell, and S. Xie, “A convnet for the 2020s,” in *Proceedings of the IEEE/CVF conference on computer vision and pattern recognition*, 2022, pp. 11 976–11 986.
- [15] C. Szegedy, S. Ioffe, V. Vanhoucke, and A. Alemi, “Inception-v4, inception-resnet and the impact of residual connections on learning,” in *Proceedings of the AAAI conference on artificial intelligence*, vol. 31, no. 1, 2017.
- [16] S. Beycimem, D. Ignatyev, and A. Zolotas, “A comprehensive survey of unmanned ground vehicle terrain traversability for unstructured environments and sensor technology insights,” *Engineering Science and Technology, an International Journal*, vol. 47, p. 101457, 2023.

- [17] T. Selvathai, J. Varadhan, and S. Ramesh, "Road and off road terrain classification for autonomous ground vehicle," in *2017 International Conference on Information Communication and Embedded Systems (ICICES)*. IEEE, 2017, pp. 1–3.
- [18] S. Sharma, J. E. Ball, B. Tang, D. W. Carruth, M. Doude, and M. A. Islam, "Semantic segmentation with transfer learning for off-road autonomous driving," *Sensors*, vol. 19, no. 11, p. 2577, 2019.
- [19] A. Valada, G. L. Oliveira, T. Brox, and W. Burgard, "Deep multi-spectral semantic scene understanding of forested environments using multimodal fusion," in *2016 international symposium on experimental robotics*. Springer, 2017, pp. 465–477.
- [20] X. Liu, J. Wang, and J. Li, "Urtsegnet: A real-time segmentation network of unstructured road at night based on thermal infrared images for autonomous robot system," *Control Engineering Practice*, vol. 137, p. 105560, 2023.
- [21] H. Xiong, W. Cai, and Q. Liu, "Mcnnet: Multi-level correction network for thermal image semantic segmentation of nighttime driving scene," *Infrared Physics & Technology*, vol. 113, p. 103628, 2021.
- [22] B. Graham, M. Engelcke, and L. Van Der Maaten, "3d semantic segmentation with submanifold sparse convolutional networks," in *Proceedings of the IEEE conference on computer vision and pattern recognition*, 2018, pp. 9224–9232.
- [23] J. Bae, J. Seo, T. Kim, H.-G. Jeon, K. Kwak, and I. Shim, "Self-supervised 3d traversability estimation with proxy bank guidance," *IEEE Access*, 2023.
- [24] H. Lee and W. Chung, "A self-training approach-based traversability analysis for mobile robots in urban environments," in *2021 IEEE International Conference on Robotics and Automation (ICRA)*. IEEE, 2021, pp. 3389–3394.
- [25] J. Seo, T. Kim, K. Kwak, J. Min, and I. Shim, "Scate: A scalable framework for self-supervised traversability estimation in unstructured environments," *IEEE Robotics and Automation Letters*, vol. 8, no. 2, pp. 888–895, 2023.
- [26] J. Frey, D. Hoeller, S. Khattak, and M. Hutter, "Locomotion policy guided traversability learning using volumetric representations of complex environments," in *2022 IEEE/RSJ International Conference on Intelligent Robots and Systems (IROS)*. IEEE, 2022, pp. 5722–5729.
- [27] F. Ruetz, N. Lawrence, E. Hernández, P. Borges, and T. Peynot, "Forestrav: 3d lidar-only forest traversability estimation for autonomous ground vehicles," *IEEE Access*, 2024.
- [28] D. Fusaro, E. Olivastri, I. Donadi, D. Evangelista, E. Menegatti, and A. Pretto, "Pyramidal 3d feature fusion on polar grids for fast and robust traversability analysis on cpu," *Robotics and Autonomous Systems*, vol. 170, p. 104524, 2023.
- [29] H. Zhou, X. Zhu, X. Song, Y. Ma, Z. Wang, H. Li, and D. Lin, "Cylinder3d: An effective 3d framework for driving-scene lidar semantic segmentation. arxiv 2020," *arXiv preprint arXiv:2008.01550*, 2020.
- [30] C. Min, W. Jiang, D. Zhao, J. Xu, L. Xiao, Y. Nie, and B. Dai, "Orfd: A dataset and benchmark for off-road freespace detection," in *2022 international conference on robotics and automation (ICRA)*. IEEE, 2022, pp. 2532–2538.
- [31] H. Ye, J. Mei, and Y. Hu, "M2f2-net: Multi-modal feature fusion for unstructured off-road freespace detection," in *2023 IEEE Intelligent Vehicles Symposium (IV)*. IEEE, 2023, pp. 1–7.
- [32] J. Li, Y. Zhan, P. Yun, G. Zhou, Q. Chen, and R. Fan, "Roadformer: Duplex transformer for rgb-normal semantic road scene parsing," *IEEE Transactions on Intelligent Vehicles*, 2024.
- [33] J. Seo, T. Kim, S. Ahn, and K. Kwak, "Metaverse: Meta-learning traversability cost map for off-road navigation," *arXiv preprint arXiv:2307.13991*, 2023.
- [34] J. Seo, S. Sim, and I. Shim, "Learning off-road terrain traversability with self-supervisions only," *IEEE Robotics and Automation Letters*, 2023.
- [35] L. Wellhausen, A. Dosovitskiy, R. Ranftl, K. Walas, C. Cadena, and M. Hutter, "Where should i walk? predicting terrain properties from images via self-supervised learning," *IEEE Robotics and Automation Letters*, vol. 4, no. 2, pp. 1509–1516, 2019.
- [36] O. Ronneberger, P. Fischer, and T. Brox, "U-net: Convolutional networks for biomedical image segmentation," in *Medical image computing and computer-assisted intervention—MICCAI 2015: 18th international conference, Munich, Germany, October 5-9, 2015, proceedings, part III 18*. Springer, 2015, pp. 234–241.
- [37] K. He, X. Zhang, S. Ren, and J. Sun, "Deep residual learning for image recognition," in *Proceedings of the IEEE conference on computer vision and pattern recognition*, 2016, pp. 770–778.
- [38] C. Choy, J. Gwak, and S. Savarese, "4d spatio-temporal convnets: Minkowski convolutional neural networks," in *Proceedings of the IEEE/CVF conference on computer vision and pattern recognition*, 2019, pp. 3075–3084.
- [39] J. Cabrera, A. Santo, A. Gil, C. Viegas, and L. Payá, "Minkunext: Point cloud-based large-scale place recognition using 3d sparse convolutions," *arXiv preprint arXiv:2403.07593*, 2024.
- [40] J. Komorowski, "Minkloc3d: Point cloud based large-scale place recognition," in *Proceedings of the IEEE/CVF Winter Conference on Applications of Computer Vision*, 2021, pp. 1790–1799.
- [41] G. Larsson, M. Maire, and G. Shakhnarovich, "Fractalnet: Ultra-deep neural networks without residuals," *CoRR*, vol. abs/1605.07648, 2016. [Online]. Available: <http://arxiv.org/abs/1605.07648>
- [42] D. Hendrycks and K. Gimpel, "Bridging nonlinearities and stochastic regularizers with gaussian error linear units," *CoRR*, vol. abs/1606.08415, 2016. [Online]. Available: <http://arxiv.org/abs/1606.08415>
- [43] J. Behley, M. Garbade, A. Milioto, J. Quenzel, S. Behnke, J. Gall, and C. Stachniss, "Towards 3D LiDAR-based semantic scene understanding of 3D point cloud sequences: The SemanticKITTI Dataset," *The International Journal on Robotics Research*, vol. 40, no. 8-9, pp. 959–967, 2021.
- [44] A. Geiger, P. Lenz, and R. Urtasun, "Are we ready for autonomous driving? the kitti vision benchmark suite," in *2012 IEEE conference on computer vision and pattern recognition*. IEEE, 2012, pp. 3354–3361.
- [45] P. Jiang, P. Osteen, M. Wigness, and S. Saripalli, "Rellis-3D dataset: Data, benchmarks and analysis," in *2021 IEEE Int. Conf. on robotics and automation (ICRA)*. IEEE, 2021, pp. 1110–1116.
- [46] P. Jiang and S. Saripalli, "Lidarnet: A boundary-aware domain adaptation model for point cloud semantic segmentation," in *2021 IEEE Int. Conf. on Robotics and Automation (ICRA)*. IEEE, 2021, pp. 2457–2464.
- [47] S. Xie, R. B. Girshick, P. Dollár, Z. Tu, and K. He, "Aggregated residual transformations for deep neural networks," *CoRR*, vol. abs/1611.05431, 2016. [Online]. Available: <http://arxiv.org/abs/1611.05431>
- [48] K. He, X. Zhang, S. Ren, and J. Sun, "Deep residual learning for image recognition," *CoRR*, vol. abs/1512.03385, 2015. [Online]. Available: <http://arxiv.org/abs/1512.03385>
- [49] S. Ioffe and C. Szegedy, "Batch normalization: Accelerating deep network training by reducing internal covariate shift," in *International conference on machine learning*. pmlr, 2015, pp. 448–456.
- [50] J. L. Ba, J. R. Kiros, and G. E. Hinton, "Layer normalization," *arXiv preprint arXiv:1607.06450*, 2016.
- [51] C. R. Qi, H. Su, K. Mo, and L. J. Guibas, "Pointnet: Deep learning on point sets for 3d classification and segmentation," in *Proceedings of the IEEE conference on computer vision and pattern recognition*, 2017, pp. 652–660.
- [52] C. R. Qi, L. Yi, H. Su, and L. J. Guibas, "Pointnet++: Deep hierarchical feature learning on point sets in a metric space," *Advances in neural information processing systems*, vol. 30, 2017.
- [53] C. Xu, B. Wu, Z. Wang, W. Zhan, P. Vajda, K. Keutzer, and M. Tomizuka, "Squeezesegv3: Spatially-adaptive convolution for efficient point-cloud segmentation," in *Computer Vision—ECCV 2020: 16th European Conference, Glasgow, UK, August 23–28, 2020, Proceedings, Part XXVIII 16*. Springer, 2020, pp. 1–19.
- [54] T. Cortinhal, G. Tzelepis, and E. Erdal Aksoy, "Salsanext: Fast, uncertainty-aware semantic segmentation of lidar point clouds," in *Advances in Visual Computing: 15th International Symposium, ISVC 2020, San Diego, CA, USA, October 5–7, 2020, Proceedings, Part II 15*. Springer, 2020, pp. 207–222.
- [55] A. Milioto, I. Vizzo, J. Behley, and C. Stachniss, "Rangenet++: Fast and accurate lidar semantic segmentation," in *2019 IEEE/RSJ international conference on intelligent robots and systems (IROS)*. IEEE, 2019, pp. 4213–4220.
- [56] Y. Hou, X. Zhu, Y. Ma, C. C. Loy, and Y. Li, "Point-to-voxel knowledge distillation for lidar semantic segmentation," in *Proceedings of the IEEE/CVF conference on computer vision and pattern recognition*, 2022, pp. 8479–8488.
- [57] Z. Liu, Y. Lin, Y. Cao, H. Hu, Y. Wei, Z. Zhang, S. Lin, and B. Guo, "Swin transformer: Hierarchical vision transformer using shifted windows," in *Proceedings of the IEEE/CVF international conference on computer vision*, 2021, pp. 10012–10022.